Eur. Phys. J. B **59**, 127–132 (2007)
DOI: 10.1140/epjb/e2007-00260-x

THE EUROPEAN PHYSICAL JOURNAL B

Speed of adaptation in structured populations

E. de A. Gonçalves[1], V.M. de Oliveira[1,a], A. Rosas[2,b], and P.R.A. Campos[3,c]

[1] Departamento de Estatística e Informática, Universidade Federal Rural de Pernambuco, 52171-900, Dois Irmãos, Recife, PE, Brazil
[2] Departamento de Física, CCEN, Universidade Federal da Paraíba, Caixa Postal 5008, 58051-970, João Pessoa, PB, Brazil
[3] Departamento de Física, Universidade Federal Rural de Pernambuco, 52171-900, Dois Irmãos, Recife, PE, Brazil

Received 12 February 2007 / Received in final form 9 August 2007
Published online 5 October 2007 –

Abstract. Adaptation of populations takes place with the occurrence and subsequent fixation of mutations that confer some selective advantage to the individuals which acquire it. For this reason, the study of the process of fixation of advantageous mutations has a long history in the population genetics literature. Particularly, the previous investigations aimed to find out the main evolutionary forces affecting the strength of natural selection in the populations. In the current work, we investigate the dynamics of fixation of beneficial mutations in a subdivided population. The subpopulations (demes) can exchange migrants among their neighbors, in a migration network which is assumed to have either a random graph or a scale-free topology. We have observed that the migration rate drastically affects the dynamics of mutation fixation, despite of the fact that the probability of fixation is invariant on the migration rate, accordingly to Maruyama's conjecture. In addition, we have noticed a topological dependence of the adaptive evolution of the population when clonal interference becomes effective.

PACS. 87.23.Kg Dynamics of evolution – 87.15.Aa Theory and modeling; computer simulation

1 Introduction

Adaptation in microbe populations, in the simplest scenario, consists of rare beneficial mutations which through rapid selective sweeps reach fixation in the population [1]. These fixation events are alternated by periods of low activity, where no beneficial mutation is fixed. Although the occurrence of deleterious mutations are much more likely, this simplistic view can be broken down for very large population sizes or high mutation rates. Upon these circumstances, the coexistence of distinct beneficial mutations becomes common. In asexual populations, where genomes carrying distinct mutations can not recombine to form a better adapted entity, this leads to a strong competition between distinct beneficial mutations in order to reach fixation with the ultimate loss of the remaining ones, a phenomenon which is known as clonal interference [2]. The clonal interference results in longer fixation times and consequently a slower adaptation rate in asexual populations.

The phenomenon of clonal interference has been extensively studied for a long term in both theoretical [3–7] and experimental frameworks [5,8–12]. Those investigations upgraded the understanding of the evolutionary mechanisms affecting the clonal interference strength in natural populations. Despite of the advances, those investigations were restricted to the assumption of non-structured populations. A first attempt to tackle the problem of structured populations was the analysis of the advantageous mutations fixation dynamics in a spatially structured asexual haploid population [13,14]. In that model, the individuals were distributed in a two-dimensional lattice with local competition, i.e., the organisms interacted only with their nearest neighbors. It was shown that the beneficial mutation substitution rate in a spatially structured population is smaller than the one observed in non-structured populations. This is more pronounced as the adaptive mutation rate increases, exactly where clonal interference becomes more relevant [13].

However, to our knowledge, the role of network topology and structuring on the adaptive process of subdivided populations has not been analyzed yet, perhaps because of the belief that population structure does not influence the population dynamics. In fact, Maruyama has demonstrated that under certain types of population structure, more specifically models that assume conservative migration, the fixation probability of adaptive mutations is the same as in an undivided population [15]. This is precisely what we have observed in our model as long as neither

[a] e-mail: viviane@deinfo.ufrpe.br
[b] e-mail: arosas@fisica.ufpb.br
[c] e-mail: paulo.campos@df.ufrpe.br

extinction nor clonal interference are considered. Therefore, this contribution focuses on the competition between different clones for fixation, how it changes this scenario, and how topology affects the competition.

To this end, we consider a structured population model recently introduced to investigate patterns of neutral genetic variation in the epidemiological context of susceptible-infected-susceptible model (SIS) [16,17]. Here, the model is slightly modified such that the individuals are subjected to natural selection.

The paper is organized as follows: Section 2 describes the model. In Section 3 we show our simulation results, and finally in Section 4 we present our conclusions.

2 The model

Recently, Gordo and Campos introduced a structured population model to describe pathogen diversity evolution [16,17]. In their model the population is subdivided in several small sub-populations called *demes*. Each deme can exchange migrants with their neighbor demes. We assume two distinct topologies for this migration network: random graphs [18] and scale-free networks [19]. The total number of demes in the population is D, and each deme can carry N_d individuals, hence, the maximum population size is $N = DN_d$. Each deme might be extinct with probability e at each generation. By extinction we mean that the deme becomes empty, but the deme can be recolonized through migration. At each generation the number of migrants of a given deme is taken from a Poisson distribution of mean $N_d m k_j$, where m is the migration rate per link per individual and k_j is the connectivity of deme j. The emigrants are randomly chosen among the N_d individuals in the deme and moved to one of the k_j demes.

Opposed to the original model, where neutral selection was assumed [16], we consider natural selection. We also assume the occurrence of both beneficial and deleterious mutations, which occurs at rates U_b and U_d, respectively. The net selective effect s_b of a given beneficial mutations is exponentially distributed, except when otherwise stated, according to

$$P(s_b) = \beta \exp(-\beta s_b) \tag{1}$$

where $1/\beta$ is the mean selective effect of advantageous mutations [20]. On the other hand, each deleterious mutation reduces the adaptation value of the organisms by a constant factor $(1 - s_d)$. Hence, the adaptation of an individual with k_b beneficial mutations and k_d deleterious mutations is

$$\omega = \left[\prod_{i=1}^{k_b}(1 + s_b(i))\right](1 - s_d)^{k_d}. \tag{2}$$

The ultimate fate of any mutation is either its fixation or its loss from the population. A fixation event occurs when all individuals in the population have acquired that mutation. The rate of fixation is then calculated by measuring the number of fixation events in a given time window divided by the size of this time interval.

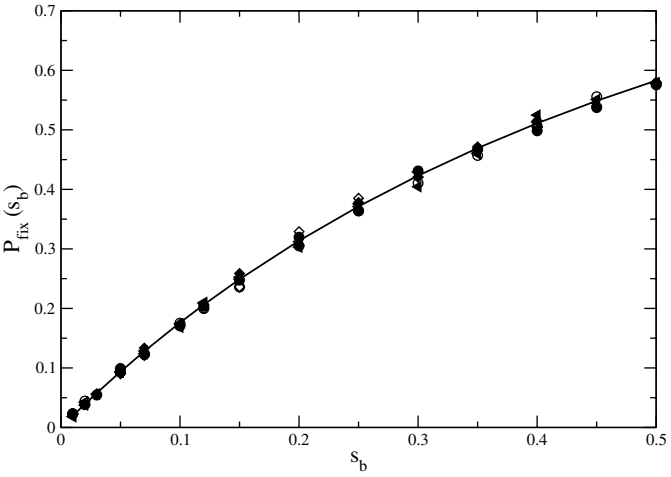

Fig. 1. Fixation probability P_{fix} as a function of the selective benefit s_b of the beneficial mutation. The data correspond to results from 5000 runs. The parameters are $N = 10\,000$, $D = 200$, $U_d = 0$, $e = 0$, and $m = 0.0001$ (left triangles), $m = 0.001$ (diamonds) and $m = 0.01$ (circles). The filled symbols correspond to the results for the random graph simulations, whereas open symbols refer to scale-free topologies. In both cases the mean connectivity of the network is $z = 6$. The thick line is the theoretical prediction for a homogeneous population according to equation (3).

3 Results

Maruyama has claimed that upon conservative migration, i.e. the expected number of emigrants equals the number of immigrants in a deme, the probability of fixation is not dependent on the population structure and it is the same as in a homogeneous population [15]. In order to test this hypothesis in our model, we have measured the fixation probability of advantageous mutations as a function of their benefit effect s_b. Starting the population with $N - 1$ individuals whose fitnesses are equal to one and a single mutant with fitness $1 + s_b$ (here s_b is fixed instead of exponentially distributed), we have recorded the fate of that beneficial mutation. At this stage, there is no competition among beneficial mutations and the extinction rate has been settled to zero. This corresponds to the celebrated two-allele model [23]. In Figure 1 we show the fixation probability (the number of instances where fixation has been achieved divided by the number of samples) as a function of s_b for several migration rates and different topologies (random graphs and scale-free networks), but with the same mean connectivity. It is worth mentioning that Maruyama's hypothesis does not consider neither competition among advantageous mutations nor extinction of demes. In the figure we also compare our results with that expected in a homogeneous population, which is the solution of the following equation

$$P_{fix} = 1 - e^{-(1+s_b)P_{fix}}, \tag{3}$$

obtained by means of the branching process formulation [24] for the fixation probability in a homogeneous

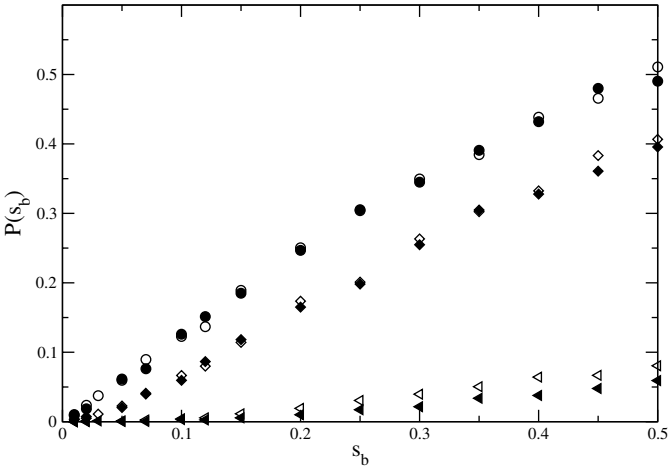

Fig. 2. Fixation probability P_{fix} as a function of the selective benefit s_b of the beneficial mutation. The simulation parameters are the same as in Figure 1, except that $e = 0.02$.

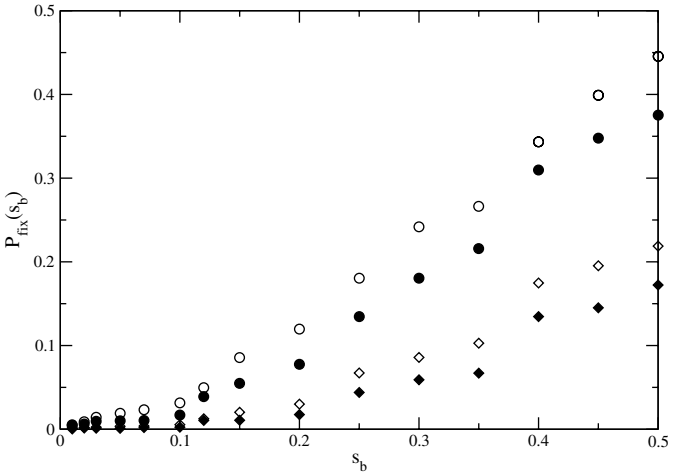

Fig. 3. The effect of deleterious mutations on the fixation probability P_{fix}. The simulation parameters are $N = 10\,000$, $D = 200$, $U_d = 0.1$, $s_d = 0.1$, $e = 0$, and $m = 0.001$ (diamonds) and $m = 0.01$ (circles). The filled symbols denote the random graph topology, whereas empty symbols represent scale-free networks.

population [23]. The collapse of all curves indicates that Maruyama's assumption is indeed valid in this case.

On the other hand, in Figure 2 we show the fixation probability as a function of s_b but now there is a non-null extinction probability. Conversely, we now see that there is a clear dependence on the migration rate m. We also observe a topological dependence, especially for low migration rates, where the fixation probability in a scale-free network is slightly greater than in a random graph. We also observe that the fixation probability increases with the migration rate. What is more, for very small migration rate, the beneficial mutation will disappear before it can migrate, thence there will be no fixation at all.

In Figure 3 we investigate the joint effect of deleterious and beneficial mutations on the fixation probability of the latter ones. The parameters are the same as in Figure 1, except that now $U_d = 0.1$ and $s_d = 0.1$. In spite of conservative migration, since $e = 0$, we see that now the probability of fixation is dependent on the migration rate, opposed to the case $U_d = 0$. More specifically, we find that a smaller migration rate leads to a smaller probability of fixation. We argue that this behavior is a consequence of the dependence of the time a mutation takes to fix on the migration rate. Although the fixation probability of a single beneficial mutation is the same for all values of migration rate, as shown in Figure 1, its fixation time is noticeably dependent on m. For large m the mutation can rapidly spread all over the deme network, whereas for small m the process of diffusion over the population is very slow. However, long fixation times allows the appearance of more segregating deleterious mutations, which reduces adaptation, and consequently the chance of fixation is greatly affected. As expected, we also observe that the probability of fixation decreases with the augment of U_d [6,21,22] (results not shown) and that U_d enhances the topological effects.

None of these previous simulations conceive competition among distinct advantageous mutations. Consequently it is not possible to appreciate how other evolutionary factors such as clonal interference can affect the evolutionary dynamics. From now on, we will assume that beneficial mutations take place at a constant rate U_b. We will start the simulations by assuming a population of individuals which are mutation-free. We then let the population evolve until $N_{ev} = 20$ fixation events have occurred and estimate the number of generations that it takes. The process is repeated N_{runs} times in order to get a reasonable statistical confidence on our simulation results. We have ascertained that $N_{runs} = 50$ provides a good statistics for the data. In Figure 4 we plot the beneficial mutation fixation rate R_b as a function of the rate of advantageous mutations, U_b, for some values of m and for the two topologies under consideration, random graphs and scale-free networks. In this figure $e = 0$ and so there is no clearance of the demes (extinction). As expected, we clearly notice that the fixation rate increases with the augment of U_b, and R_b is strongly dependent on the migration rate m. A smaller migration rate means effectively a smaller fixation rate R_b. Again, this is closely related to the dependence of the time a beneficial mutation takes for fixation with the migration rate. We also notice that the rate of growth of R_b decreases as a smaller migration rate is considered. From the figure, a dependence of R_b on the topology of the interaction network is observed, R_b being larger for scale-free than for random graphs networks. However, the differences between the two topologies is only pronounced in the regime of large U_b. In this regime, a large supply of beneficial mutations results in a strong competition among the distinct mutations, and so the occurrence of clonal interference. Consequently, the fixation of a given mutation means the ultimate loss of all its competitors.

Together with the simulation results, we also show the expected fixation rate in a infinitely large homogeneous population disregarding the clonal interference, which is

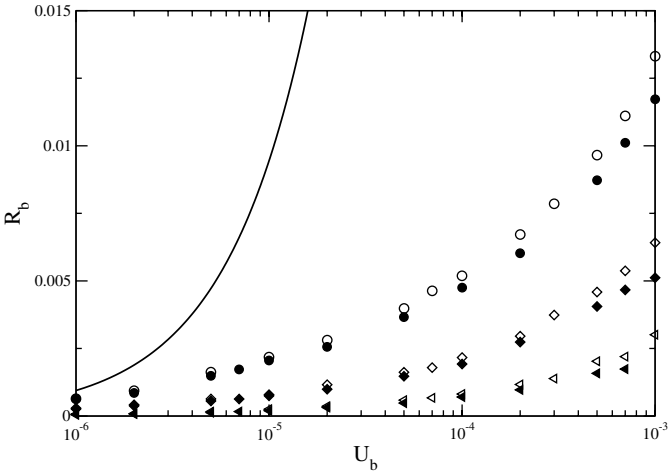

Fig. 4. Fixation rate of beneficial mutations as a function of the mutation rate U_b. The parameters used in the simulation are $N = 10\,000$, $D = 200$, $U_d = 0$, $e = 0$, $\beta = 20$, $z = 4$, and $m = 0.0001$ (left triangles), $m = 0.001$ (diamonds) and $m = 0.01$ (circles). The filled data points corresponds to the simulation results for random graph networks, whereas empty data points refer to scale-free topologies. The thick line is the expected rate for a homogeneous population without clonal interference given by equation (4).

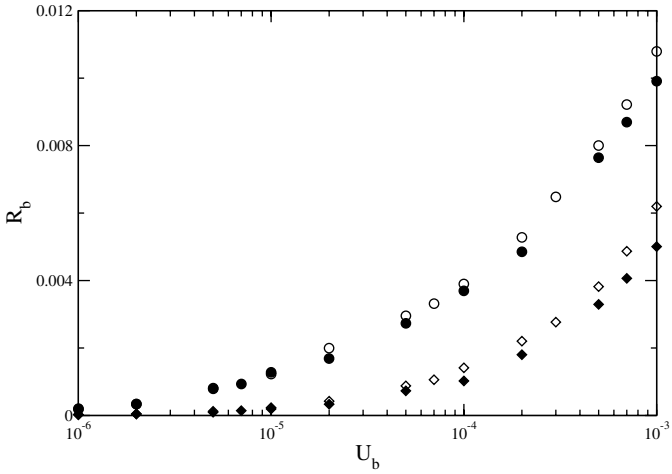

Fig. 5. Fixation rate of beneficial mutations as a function of the mutation rate U_b. The simulation parameters are the same as in Figure 4, except that $e = 0.02$.

given by (see Ref. [4])

$$k_b = NU_bP_{fix}(\beta), \tag{4}$$

where NU_b is the number of beneficial mutations per generation and $P_{fix}(\beta)$ is the fixation probability of a given beneficial mutation whose selective effect is exponentially distributed[1]. For small U_b, where clonal interference is not so strong, the fixation rate for a homogeneous population is not very distinct from our simulation results for structured populations. However, as U_b increases and competition among beneficial mutations becomes common, equation (4) clearly overestimates the simulation results.

In Figure 5 we show the fixation rate R_b as a function of the mutation rate U_b for $U_d = 0$ and a non-null extinction rate, $e = 0.02$. Therefore, for this specific value of the extinction rate, at each $t = 50$ generations, in average, each deme goes through an extinction process, which means that the deme becomes empty. In subsequent generations the extincted deme can be recolonized by migrants from neighbor demes. We observe the same qualitative scenario as in Figure 4. As in the previous case (without extinction), the difference between the rates for random graphs and scale-free networks is clearly observed in the clonal interference regime. Nevertheless, when extinction is at work, the fixation rate decreases.

For the sake of completeness, in Figure 6 we plot the fixation rate for fixed migration rate m and distinct values of deleterious mutations rate U_d. As expected, the rate R_b decreases as we increase the mutation rate U_d, because of a smaller fixation probability. Besides, the same qualitative scenario is seen and once more scale-free networks display a higher performance than random graphs for the rate of substitution of the advantageous mutations.

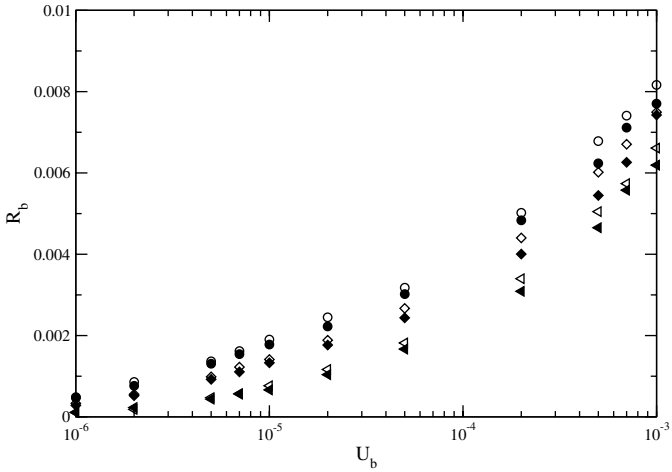

Fig. 6. The effect of deleterious mutations on the fixation rate of advantageous mutations. The parameters used in the simulations are $N = 10\,000$, $D = 200$, $m = 0.001$, $s_d = 0.1$, $e = 0$, $\beta = 20$, $z = 4$, and $U = 0.01$ (circles), $U = 0.05$ (diamonds) and $U = 0.1$ (left triangles). The filled data points corresponds to random graph simulations, whereas empty data points refer to scale-free topologies.

3.1 Dynamics of non-fixed mutations

Recently, Rosas et al. [25] have investigated the dynamics of favorable mutations loss in an asexual population. They have focused their study on the analysis of the probability distribution, $P(s)$, of the maximum population size achieved by mutations before they reach extinction due to

[1] We have estimated the probability of fixation $P_{fix}(\beta)$ by means of equation (3), and because the selective effects of favorable mutations are exponentially distributed, we have numerically integrated the solution provided in the previous step over all possible values of selective effects.

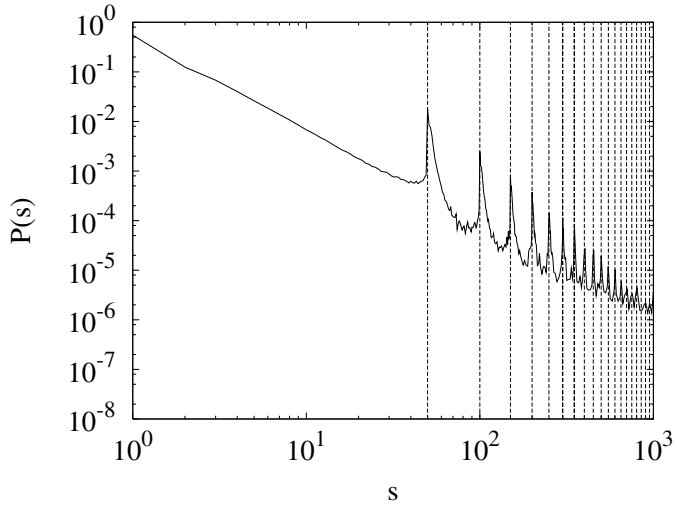

Fig. 7. Probability distribution of maximum population sizes reached by mutations that have subsequently been lost. The parameters are $N = 10\,000$, $D = 200$, $z = 4$, $m = 0.0001$ and $e = 0$. The vertical lines indicate multiples of the deme size (50 in this case).

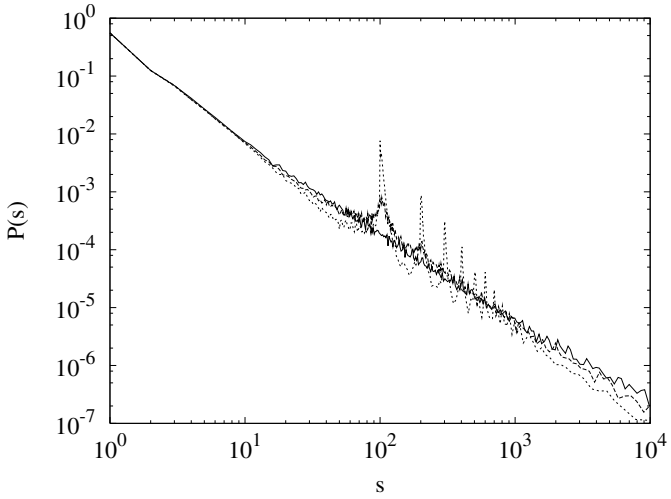

Fig. 8. Probability distribution of maximum population sizes reached by mutations that have subsequently been lost. The parameters are $N = 20\,000$, $D = 200$, $z = 4$, $e = 0$ and $m = 0.01$ (solid line), $m = 0.001$ (dashed-line) and $m = 0.0001$ (short-dashed line).

genetic drift or to clonal interference. Interestingly, they showed that two distinct scaling emerge from the analysis of $P(s)$: one for small s, where genetic drift is the main evolutionary force and clonal interference has a subtler role, and another for large population size s, where clonal interference prevails over the genetic drift. This analysis is particularly elucidating because it allows the quantitative determination of the regions where clonal interference and genetic drift are dominant without any a priori assumption.

Here we have also analyzed the probability distribution $P(s)$ in order to get some insight about the dynamics of the beneficial mutations fixation in a structured population. Figure 7 shows $P(s)$ for a structured population composed of $N = 10\,000$ individuals which are subdivided in $D = 200$ demes. Opposed to what was observed in a homogeneous and in spatially distributed populations [25], the distribution $P(s)$ is characterized by the occurrence of several peaks distributed over an almost straight line in a log-log plot. We also check that these peaks manifest around integer multiples of the deme size $N_d = 50$.

In Figure 8 we have increased the deme size to $N_d = 100$ and we see once again that the peaks in the distribution takes place at multiples of the deme size. Nevertheless, in Figure 8 we also observe that an augment of the migration rate m reduces the amplitude of the peaks, and for very large m the peaks are no longer noticeable. Since the time that a given individual takes to move from the original deme to one of the neighbors demes is proportional to $1/m$, at low migration rates this time is too long compared to the time a given advantageous mutation spends to reach fixation in a deme. Therefore, a given beneficial mutation can escape drift and reach fixation in the deme it has been originated or it simply becomes lost in the earlier stages of its appearance. If the beneficial mutation has been successful, it can move to another neighbor deme and now has to compete for fixation in this second deme. Naturally, its survival probability in the second deme depends on the genetic background of that deme. In a well-established population with larger beneficial mutation, its fixation will be rather unlikely. In addition, the population of the original deme can be invaded and outcompeted by more adapted mutants from neighbor demes leading to its elimination from the population. Altogether, those two effects explain the existence of the first peak. On the other hand, when the second deme population genetic background is weaker than the one of the first deme, the selective advantage of the first deme population may lead to the domination of the second deme. This reasoning can be pursued to explain the other peaks as well as the beneficial mutation spread over the whole population and its ultimate fixation.

For high migration rates, the time that a given mutation takes to move from one deme to another is very short, which means that as soon as an advantageous mutation arises and it starts to grow in size, a rapid spreading of the mutation over the whole network and the process of fixation is faster. Consequently, the peaks in $P(s)$ disappear.

4 Conclusions

We have studied the evolutionary dynamics in a structured population model introduced by Campos and Gordo [16], where the population is subdivided in several small subpopulations that exchange individuals by migration. Differently of the original model, here we have assumed that the individuals are subjected to the influence of natural selection. We have considered two distinct topologies for the migration network: random graphs and scale-free networks. As expected from Maruyama's claim,

the fixation probability of a given beneficial mutation is not influenced by neither the rate at which individuals move from one deme to the other nor by the topology of the network in the absence of deleterious mutations and extinction. The same is not true when extinction occurs, since extinction creates an asymmetry in the probability of emigration and immigration. Similarly, when deleterious mutations are taken into account we find a strong dependence on the migration rate even for null extinction rate. What is more, in the presence of extinction or deleterious mutations the probability of fixation depends on the topology.

By letting the population evolve in a given time window we were able to measure the fixation rate of beneficial mutations for a given mutation rate U_b. As usual, the rate R_b is an increasing function of the mutation rate U_b. We have seen that R_b is fairly dependent on the migration rate, with a greater migration resulting in an acceleration of the adaptive process. In spite of the independence of the fixation probability of a given mutation on the migration rate, the time it takes to spread over the whole population is proportional to $1/m$. This essential part of the dynamics is captured when we measure the rate of substitutions, even when the extinction rate is null. Nicely, we have also observed that the topology of the network affects the evolutionary dynamics of the population in the regime of large mutation rates U_b, which is exactly the regime where clonal interference becomes more effective. More specifically, the scale-free topology presents a faster adaptation speed than random graphs. This result is particularly important because it demonstrates that pathogen population dynamics should also be taken into account in the studies of the interchange of network topologies and disease dynamics [26–29].

Finally, the analysis of the distribution of beneficial mutations extincted before fixation shed light over the dynamics of advantageous mutations diffusion. For low migration rates (slow diffusion) the distribution $P(s)$ presents peaks on multiples of deme size, while for large migration rates (fast diffusion) the evolution of the system is more uniform and the peaks disappear.

PRAC, VMO and AR are supported by Conselho Nacional de Desenvolvimento Científico e Tecnológico (CNPq). EAG is grateful to Pedro de Sá for the useful comments.

References

1. K.C. Atwood, L.K. Schneider, F.J. Ryan, Proc. Natl. Acad. Sci. USA **37**, 146 (1951)
2. W.G. Hill, A. Robertson, Genet. Res. **8**, 269 (1966)
3. P.R.A. Campos, V.M. de Oliveira, Evolution **58**, 932 (2004)
4. V.M. de Oliveira, P.R.A. Campos, Physica A **337**, 546 (2004)
5. P.J. Gerrish, R.E. Lenski, Genetica **102**, 127 (1998)
6. H.A. Orr, Genetics **155**, 961 (2000)
7. O.F.F. Raposo, A.W.S. de Almeida, A.J.F. Souza, P.R.A. Campos, Eur. Phys. J. B **50**, 653 (2006)
8. J.M. Cuevas, S.F. Elena, A. Moya, Genetics **162**, 533 (2002)
9. R. Miralles, P.J. Gerrish, A. Moya, S.F. Elena, Science **285**, 1745 (1999)
10. R.E. Lenski, M.R. Rose, S.C. Simpson, S.C.M. Tadler, Amer. Nat. **138**, 1315 (1991)
11. D.E. Rozen, J.A.G.M. de Visser, P.J. Gerrish, Curr. Biol. **12**, 1040 (2002)
12. J.A.G.M. de Visser, D.E. Rozen, Genetics **172**, 2093 (2006)
13. I. Gordo, P.R.A. Campos, Genetica **127**, 217 (2006)
14. L. Perfeito, I. Gordo, P.R.A. Campos, Eur. Phys. J. B **51**, 301 (2006)
15. T. Maruyama, Genetical Research **15**, 221 (1970)
16. P.R.A. Campos, I. Gordo, J. Stat. Mech. L12003 (2006)
17. I. Gordo, P.R.A. Campos, BMC Evol. Biol. **7**, 116 (2007)
18. P. Erdos, A. Rényi, Publ. Math. Inst. Hung. Acad. Sci. **5**, 17 (1960)
19. A.-L. Barabási, R. Albert, Science **286**, 509 (1999)
20. J.H. Gillespie, *The Causes of Molecular Evolution* (Oxford University Press, Oxford, 1991)
21. T. Johnson, N.H. Barton, Genetics **162**, 395 (2002)
22. P.R.A. Campos, Bull. Math Biol. **66**, 473 (2004)
23. J.B.S. Haldane, Proc. Camb. Philol. Soc. **23**, 838 (1927)
24. T.E. Harris, *The Theory of Branching Processes* (Springer, Berlin, 1963)
25. A. Rosas, I. Gordo, P.R.A. Campos, Phys. Rev. E **72**, 012901 (2005)
26. R. Pastor-Satorras, A. Vespignani, Phys. Rev. Lett. **86**, 3200 (2001)
27. M. Barthélemy, A. Barrat, R. Pastor-Satorras, A. Vespignani, Phys. Rev. Lett. **92**, 178701 (2004)
28. M.J. Keeling, K.T.D. Eames, J.R. Soc. Interf. **2**, 295 (2005)
29. P.R.A. Campos, J. Combadão, F. Dionísio, I. Gordo, Phys. Rev. E **74**, 042901 (2006)